Inclusion of the Pauli Principle in a Deterministic Boltzmann Equation Solver for Semiconductor Devices

Sung-Min Hong [a] and Christoph Jungemann
EIT4, Bundeswehr University, 85577 Neubiberg, Germany
[a]E-mail: hi2ska2@gmail.com

***Abstract*— The Pauli principle is included in a deterministic Boltzmann solver for multi-dimensional semiconductor devices. The Newton-Raphson scheme is applied to solve the nonlinear Boltzmann equation, and it is found that the inclusion of the Pauli principle introduces no numerical problems, even for semiconductor devices. The impact of the Pauli principle is numerically investigated for a scaled SiGe HBT.**

I. Introduction

The Pauli principle limits the occupancy of a state to a single electron per spin direction. Its impact on simulation might be significant at low temperatures or in heavily-doped regions.

Inclusion of the Pauli principle into a Boltzmann equation solver is not a trivial task, especially for the device case. Its inclusion in Monte Carlo simulations is rather CPU intensive, because the complete distribution function has to be available at all times in the phase space (3D $\boldsymbol{k}$-space plus real space). In the case of the Monte Carlo method for devices, approximations have been developed in order to reduce the CPU time [1]–[3]. However, their validity is doubtful [4].

A deterministic Boltzmann solver based on the spherical harmonics expansion method [5] does not suffer from this problem, because the distribution function is inherently known at all times [6]. However, even in this scheme, the inclusion of the Pauli principle has been reported only for bulk systems [4]. In this work, the Pauli principle is included in a deterministic Boltzmann solver for devices, and its impact on simulation is numerically investigated.

II. Implementation

Several modifications of the physical models – the scattering operator, the boundary conditions, and the bandgap narrowing model – must be made in order to consider Fermi-Dirac statistics.

The Pauli principle introduces an additional factor in the scattering operator. For notational simplicity, only one scattering with the energy transfer of $\hbar\omega$ is explicitly shown in the following, however, its extension to the general case is straightforward. The scattering operator is decomposed into the in-scattering and out-scattering terms:

$$S_{l,m}(\varepsilon) = S^{in}_{l,m}(\varepsilon) - S^{out}_{l,m}(\varepsilon). \tag{1}$$

When the transition rate depends only on the relative angle between the initial and final wave vectors, the projection of the in-scattering term (a transition from $\varepsilon - \hbar\omega$ to ε) yields [7]

$$S^{in}_{l,m}(\varepsilon) = \sum_{l',m'} \sum_{l'',m''} [Z_{l'',m''}(\varepsilon) - g_{l'',m''}(\varepsilon)] \times g_{l',m'}(\varepsilon - \hbar\omega) c_{l'}(\varepsilon) a_{l,m,l',m',l'',m''}, \tag{2}$$

where Z is the (angle dependent) density-of-states, g the generalized energy distribution function which is a product of the density-of-states and the distribution function, c the coefficient for the transition rate, and $[Z - g]$ the so-called Pauli factor projected onto energy. Similarly, the projection of the out-scattering term (a transition from ε to $\varepsilon + \hbar\omega$) yields [7]

$$S^{out}_{l,m}(\varepsilon) = \sum_{l',m'} \sum_{l'',m''} [Z_{l'',m''}(\varepsilon + \hbar\omega) - g_{l'',m''}(\varepsilon + \hbar\omega)] \times g_{l',m'}(\varepsilon) c_{l''}(\varepsilon + \hbar\omega) a_{l,m,l',m',l'',m''}. \tag{3}$$

The integral of the triple product, $a_{l,m,l',m',l'',m''}$, is given by

$$a_{l,m,l',m',l'',m''} = \oint Y_{l,m} Y_{l',m'} Y_{l'',m''} d\Omega, \tag{4}$$

where $Y_{l,m}$ is a spherical harmonic. Therefore, a term like $g_{l'',m''} g_{l',m'}$ is newly introduced because of the Pauli principle, and the Boltzmann equation becomes nonlinear. In order to have quadratic convergence of the Newton-Raphson scheme like in [8], the dependence of $g_{l'',m''} g_{l',m'}$ on the electrostatic potential is considered in the Jacobian matrix.

Significant simplification can be obtained when the transition rate does not depend on the scattering angle:

$$c_l = c_0 \delta_{l,0}. \tag{5}$$

The in-scattering term is given by

$$S^{in}_{l,m}(\varepsilon) = [Z_{l,m}(\varepsilon) - g_{l,m}(\varepsilon)] \times g_{0,0}(\varepsilon - \hbar\omega) c_0(\varepsilon) Y_{0,0}. \tag{6}$$

The out-scattering term is given by

$$S^{out}_{l,m}(\varepsilon) = [Z_{0,0}(\varepsilon + \hbar\omega) - g_{0,0}(\varepsilon + \hbar\omega)] \times g_{l,m}(\varepsilon) c_0(\varepsilon + \hbar\omega) Y_{0,0}. \tag{7}$$

Note that the velocity-randomizing scattering mechanism – for example, phonon scattering with constant matrix elements – is corresponding to this case.

978-1-4244-7700-5/10/$26.00 ©2010 IEEE

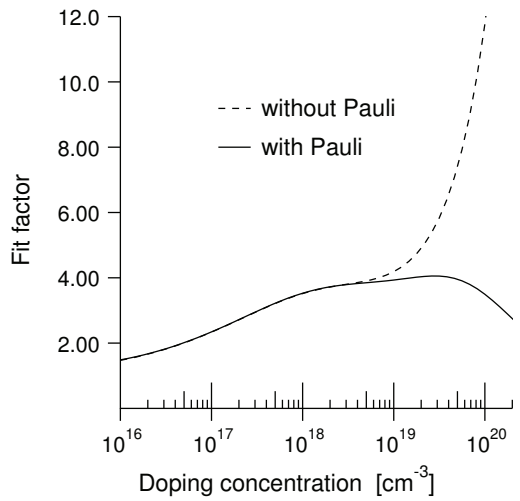

Fig. 1. Heuristic fit factor for impurity scattering with or without the Pauli principle.

Since the Brooks-Herring model for impurity scattering does not correctly describe the mobility at high doping concentrations, an empirical correction of the model is used [9]. Fig. 1 shows different fit factors used for different statistics in order to reproduce the Caughey-Thomas expression for the mobility [10]. Therefore, the mobilities limited by impurity scattering obtained from different statistics are the same.

Particle injection from the contact region is modified in order to follow Fermi-Dirac statistics. For the injection boundary condition of the Boltzmann equation we use Neumann boundary conditions together with a surface generation rate [8]

$$\Gamma^s(\boldsymbol{k}) = [f^{eq}(\boldsymbol{k})\theta(\boldsymbol{v}\cdot\boldsymbol{n}) + f(\boldsymbol{k})\theta(-\boldsymbol{v}\cdot\boldsymbol{n})]\boldsymbol{v}\cdot\boldsymbol{n}, \quad (8)$$

where $\boldsymbol{n}$ is a surface vector pointing into the device, $\theta(x)$ the step function, and $\boldsymbol{v}$ the group velocity. In the case of Fermi-Dirac statistics, f^{eq} is given by the Fermi-Dirac distribution specified by the quasi-Fermi level of the contact.

In addition to the apparent bandgap narrowing model by Klaassen $et.\ al$ [11], a correction due to Fermi-Dirac statistics is made by considering the difference of the Fermi energy obtained by the two types of statistics [12]. This correction is important because the bandgap narrowing model is consistent with Maxwell-Boltzmann statistics. The overall bandgap narrowing, ΔE, is given by

$$\Delta E = \Delta E^{Bgn} + \Delta E^{FD}, \quad (9)$$

where ΔE^{Bgn} is the apparent bandgap narrowing [11] and ΔE^{FD} is the difference of the Fermi levels for two the statistics.

III. Simulation Results

For the stabilization of the device simulation, a combination of the H-transformation and the maximum entropy dissipation scheme [13] is employed in this work [8]. In the maximum entropy dissipation scheme, the free-streaming operator is reformulated under the choice of the simplest possible entropy function, $\frac{1}{2}\exp(\frac{H}{k_BT})f^2$. The resultant free-streaming operator does not dissipate entropy at all, which should be dissipated only by scattering. Since the entropy function used in that scheme is strictly valid only for Maxwell-Boltzmann statistics, the stability of the solutions should be checked. It is found that the resultant discrete Boltzmann equation including the Pauli principle is stable even in the case of the extremely scaled SiGe HBTs shown in [14].

A two-dimensional SiGe HBT whose cutoff frequency is about 260GHz at room temperature has been simulated. The maximum doping level in the emitter region is as high as 2×10^{20}/cm^3. The analytical band model and the parameters of the related phonon scattering mechanisms proposed by the Modena group [15] have been utilized for electrons. In the case of impurity scattering an approximation by an isotropic-elastic process [9], [16] is employed. A third-order spherical harmonics expansion for the electron distribution function is used.

In Fig. 2 typical convergence behavior of the simulation is shown for different bias points. The initial solution is obtained by solving the nonlinear Boltzmann equation for a fixed electrostatic potential. Once an initial solution of the Boltzmann equation is obtained, a fully-coupled scheme is used for the Boltzmann and Poisson equations. Only when the maximum value of the potential correction at a certain Newton-Raphson iteration exceeds the energy spacing (typically 5meV in this work), additional fixed potential simulations are performed. Usually two or three iterations are sufficient to achieve a converged solution of the nonlinear Boltzmann equation, as shown in Fig. 3. When the temporal solution of the Newton-Raphson iteration is close enough to the converged solution, such fixed potential iterations naturally disappears. In every simulation the last Newton-Raphson step shows a huge decrease of the norm of the update vector.

In Fig. 4 the electron distribution function in the emitter region is shown for different Newton-Raphson iterations. In the first step its maximum value is larger than unity. However, the result of the second iteration already is very close to the Fermi-Dirac distribution.

In Fig. 5 the electron distribution function with or without the Pauli principle is shown. In the emitter region the degeneracy effect in the electron distribution function is clearly visible. However, for other regions (base and collector), the difference due to the statistics is negligible because the bandgap narrowing is modified in order to compensate it. The electron distribution function in the collector region demonstrates that our injection boundary condition [8] can handle such highly non-equilibrium distributions without any difficulties.

In Fig. 6 the electron density of the SiGe HBT is shown along the vertical position. For comparison, its counterpart for Maxwell-Boltzmann statistics is also displayed and the differences are rather small. Note that the electron density shows considerable differences without the bandgap correction, as shown in Fig. 7.

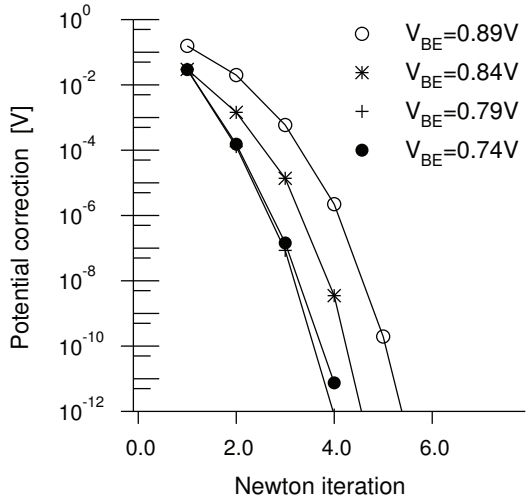

Fig. 2. Maximum value of the potential correction at each Newton-Raphson iteration for different V_{BE} values. V_{CE} = 1.2V.

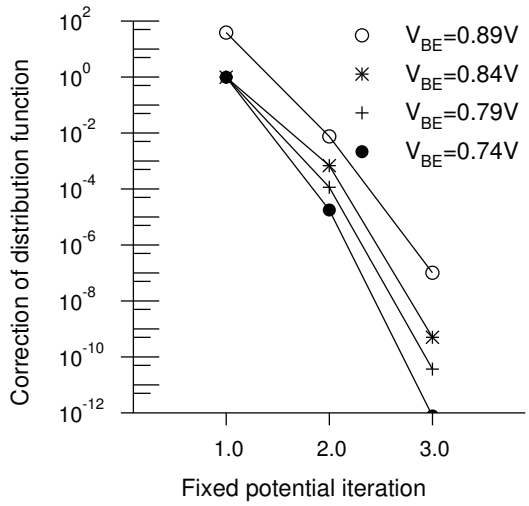

Fig. 3. Maximum value of the correction of the electron distribution function at each fixed potential iteration after the first Newton-Raphson iteration for different V_{BE} values. V_{CE} = 1.2V.

In Fig. 8 the cutoff frequency of the SiGe HBT in the quasi-stationary limit [17] is shown. Since macroscopic quantities such as the electron density agree well between the two statistics, again the impact of the Pauli principle is small, although the internal distribution function is quite different in the heavily-doped region.

IV. Conclusion

We have implemented a deterministic Boltzmann solver including the Pauli principle. Several modifications of the physical models – the scattering operator, the boundary condition, and the bandgap narrowing model – were made in order to consider Fermi-Dirac statistics. The resultant Boltzmann equation is stable and convergence degradation is not observed.

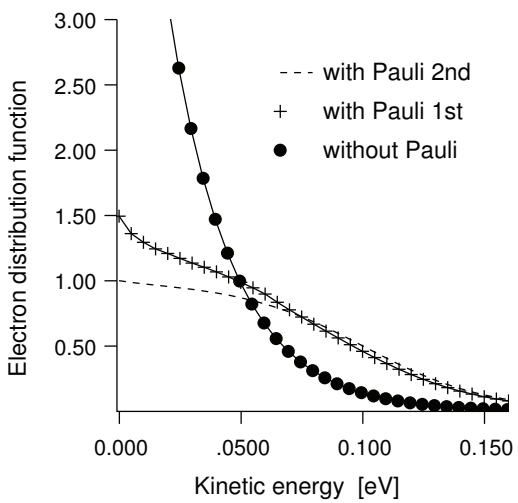

Fig. 4. Electron distribution function at the first two Newton-Raphson iterations. The values at the emitter contact are shown. V_{BE} = 0.88V and V_{CE} = 1.2V.

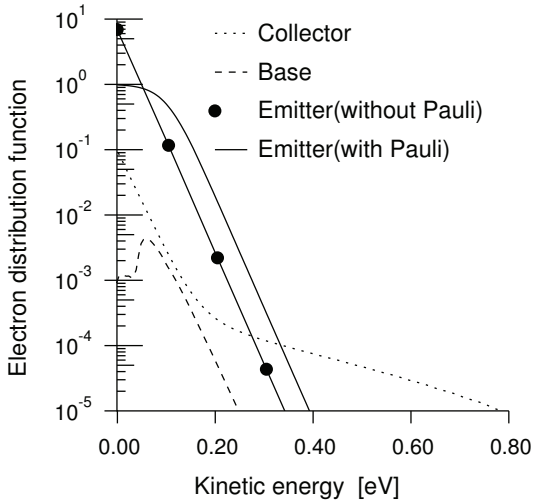

Fig. 5. Electron distribution function at different positions. V_{BE} = 0.88V and V_{CE} = 1.2V. Two values from different statistics are shown for the emitter contact. Difference due to the statistics is negligible for other points.

Acknowledgment

The research leading to these results has received funding from the Deutsche Forschungsgemeinschaft under contract number JU 406/6-1. The authors gratefully acknowledge Dr. M. Ramonas for providing the profiles of the SiGe HBT.

References

[1] M. V. Fischetti and S. E. Laux, "Monte Carlo analysis of electron transport in small semiconductor devices including band–structure and space–charge effects," *Phys. Rev. B*, vol. 38, pp. 9721–9745, 1988.

[2] J. M. M. Pantoja and J. L. S. Franco, "Monte Carlo simulation of electron velocity in degenerate GaAs," *IEEE Electron Device Lett.*, vol. 18, no. 6, pp. 258–260, 1997.

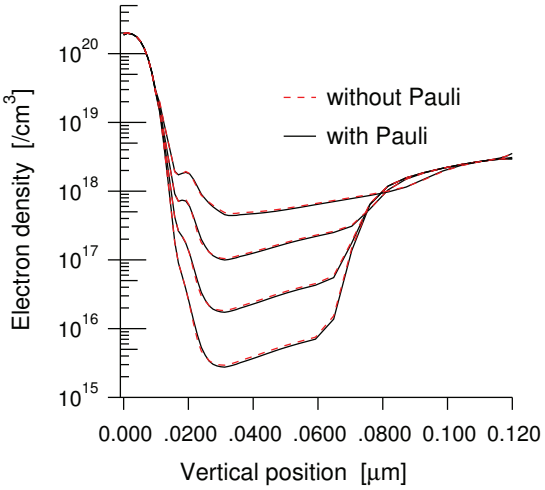

Fig. 6. Electron density along the vertical position for different V_{BE} values, 0.74V, 0.79V, 0.84V, and 0.89V. The lateral position is fixed to the center of the emitter window. V_{CE} = 1.2V.

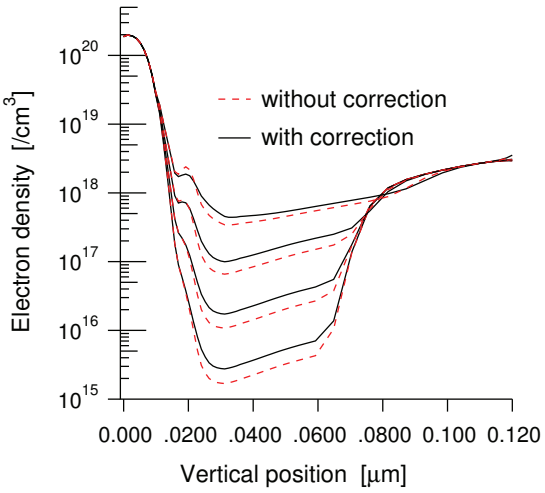

Fig. 7. Electron density obtained from simulations with or without the bandgap narrowing correction. The Pauli principle is included. Simulation condition is the same with Fig. 6.

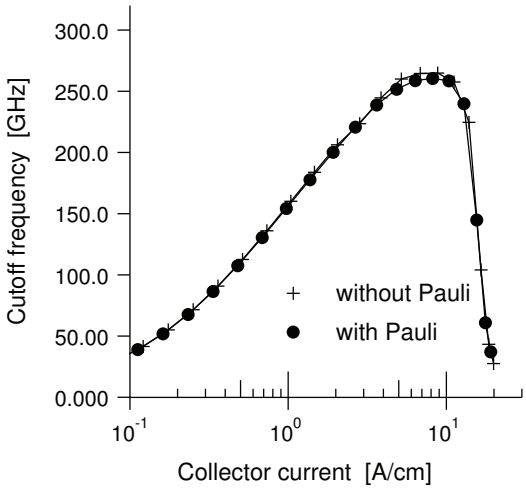

Fig. 8. Cutoff frequency of the SiGe HBT. V_{CE} = 1.2V.

[3] J. Mateos, T. González, D. Pardo, V. Hoël, H. Happy, and A. Cappy, "Improved Monte Carlo algorithm for the simulation of δ-doped AlInAs/GaInAs HEMT's," *IEEE Trans. Electron Devices*, vol. 47, no. 1, pp. 250–253, 2000.

[4] C. Jungemann, "A deterministic solver for the Langevin Boltzmann equation including the Pauli principle," in *SPIE: Fluctuations and Noise*, vol. 6600, 2007, pp. 660 007–1–660 007–12.

[5] A. Gnudi, D. Ventura, G. Baccarani, and F. Odeh, "Two-dimensional MOSFET simulation by means of a multidimensional spherical harmonics expansion of the Boltzmann transport equation," *Solid–State Electron.*, vol. 36, no. 4, pp. 575 – 581, 1993.

[6] A. J. Piazza, C. E. Korman, and A. M. Jaradeh, "A physics-based semiconductor noise model suitable for efficient numerical implementation," *IEEE Trans. Computer–Aided Des.*, vol. 18, no. 12, pp. 1730–1740, 1999.

[7] C. Jungemann, A.-T. Pham, B. Meinerzhagen, C. Ringhofer, and M. Bollhöfer, "Stable discretization of the Boltzmann equation based on spherical harmonics, box integration, and a maximum entropy dissipation principle," *J. Appl. Phys.*, vol. 100, pp. 024 502–1–13, 2006.

[8] S.-M. Hong and C. Jungemann, "A fully coupled scheme for a Boltzmann-Poisson equation solver based on a spherical harmonics expansion," *J. Computational Electronics*, vol. 8, no. 3, pp. 225–241, 2009.

[9] C. Jungemann and B. Meinerzhagen, *Hierarchical Device Simulation: The Monte-Carlo Perspective*, ser. Computational Microelectronics, S. Selberherr, Ed. Wien, New York: Springer, 2003.

[10] D. M. Caughey and R. E. Thomas, "Carrier mobilities in silicon empirically related to doping and field," *Proc. IEEE*, vol. 55, pp. 2192–2193, 1967.

[11] D. B. M. Klaassen, J. W. Slotboom, and H. C. de Graaf, "Unified apparent bandgap narrowing in *n*- and *p*-type silicon," *Solid–State Electron.*, vol. 35, pp. 125–129, 1992.

[12] L. Luo, G. Niu, and J. D. Cressler, "Modeling of bandgap narrowing for consistent simulation of SiGe HBTs across a wide temperature range," *Proc. BCTM*, pp. 123–126, 2007.

[13] C. Ringhofer, "Numerical methods for the semiconductor Boltzmann equation based on spherical harmonics expansions and entropy discretizations," *Transport Theory and Statistical Physics*, vol. 31, no. 4-6, pp. 431–452, 2002.

[14] S.-M. Hong and C. Jungemann, "Electron transport in extremely scaled SiGe HBTs," in *Proc. BCTM*, 2009, pp. 67–74.

[15] R. Brunetti, C. Jacoboni, F. Nava, L. Reggiani, G. Bosman, and R. J. J. Zijlstra, "Diffusion coefficient of electrons in silicon," *J. Appl. Phys.*, vol. 52, pp. 6713–6722, 1981.

[16] H. Kosina, "A method to reduce small-angle scattering in Monte Carlo device analysis," *IEEE Trans. Electron Devices*, vol. 46, no. 6, pp. 1196–1200, 1999.

[17] H. K. Gummel, "On the definition of the Cutoff Frequency f_T," *Proc. IEEE*, p. 2159, 1969.